Chapter 4

Electromechanical Co-Simulation for Ball Screw Feed Drive System

Liang Luo and Weimin Zhang

Additional information is available at the end of the chapter

http://dx.doi.org/10.5772/intechopen.80716

Abstract

Ball screw feed drive system is the most widely used linear drive system in the field of industrial automation. The continuous search for efficiency puts forward higher requests to the machine tool for high speed and high acceleration, which makes the feed drive system of lightweight-designed and large-size machine tools more likely to produce vibration during high-speed and high-acceleration feed operation. Electromechanical co-simulation for ball screw feed drive dynamics is an important technique for solving vibration problems occurring in the feed motion. This chapter elaborates on this technology from three aspects: modeling and simulation of dynamic characteristics of ball screw feed drive, modeling and simulation of servo control system, and the electromechanical co-simulation of ball screw feed drive system. In this chapter, the basic theoretical models, the establishment of simulation models and the comparison between simulation and experiment results of ball screw feed drive system are comprehensively introduced to provide technical references for readers.

Keywords: ball screw feed drive system, dynamic characteristics, electromechanical co-simulation, vibration, lumped mass model

1. Introduction

Ball screw feed system is the most widely used linear drive system in the field of industrial automation [1]. In order to enhance the speed and accuracy of present systems further, current research focuses on the vibration reduction and avoidance of the feed drive. Additional damping modules or structures are integrated in the feed drive system to achieve this goal, such as semi-active damping system, set point filtering, etc. Active damping system only reacts once a vibration is present, and set point filtering can lead to path deformation [2–4]. Another

way to solve this problem is to generate a smoother trajectory. For this purpose, numbers of trajectory algorithms are found out, and the frequency contents of the trajectory orders are discussed and compared [5, 6]. The vibration caused by the trajectory is difficult to analyze on hardware because of the coupling factor of variety excitation sources. All these researches need a simulation method to help the researchers or engineers study or optimize the design and parameter setting of the feed drive system [10].

Finite element model of ball screw feed drive system can predict the accurate dynamic characteristics. However, it is difficult to integrate with the simulation model of servo control system. Lumped parameter model of ball screw feed drive system can simplify the simulation model by reducing the number of degrees of freedom (DOF) of the whole system. More importantly, it can easily integrate with the simulation model of the servo control system. A reasonable simplification of the lumped parameter model is the key to accurately predict the vibration of feed drive system [7–9].

In this chapter an electromechanical co-simulation method for ball screw feed drive system was established, which can be used to study the dynamic characteristics and vibration behavior of the feed drive system. An optimized dynamic modeling and simulation method of a ball screw feed drive based on the lumped mass model was firstly presented, and the optimized calculation method of the equivalent parameters was given. Then, a model of servo control system was built up, and based on it, the electromechanical co-simulation of ball screw feed drive system was established. Finally, a simulative and experimental test is conducted based on a ball screw feed drive system test bench. The result shows that electromechanical co-simulation of ball screw feed drive system could achieve a very good predictability.

2. Dynamic characteristic modeling and simulation of ball screw feed system

2.1. Lumped mass model of ball screw feed system

A typical ball screw feed system consists of a servomotor, coupling, ball screw, work table, and base (**Figure 1**). The ball screw is supported by two sets of bearing, which are fixed to the base. The servomotor torque is transmitted through a coupling onto the ball screw shaft to drive the work table. The linear guideway constrains the movement of the work table in an axial direction. The base is fixed on the machine bed or placed on the ground. The transformation from the rotational movement of the screw shaft into the linear motion of the work table is realized by the ball screw system with its transmission ratio i, which is defined as the distance of travel h during one revolution of the shaft as the following:

$$i = \frac{h}{2\pi} \tag{1}$$

Low-order modes are the main factors affecting the dynamic characteristics of the ball screw feed drive system of machine tools. Typically, the first axial and rotational modes of the ball screw show a dominant influence on the overall dynamics, while the relevance of higher-order modes for most technical applications is rather small [8].

The lumped mass model can reasonably reduce the number of degrees of freedom (DOF) of the simulation model while preserving the low-order modes of the system to simplify calculations. **Figure 2** shows the lumped mass model of a ball screw feed drive system. The influence of the shaft on the rotational mode and axial mode of the drive system is explicitly included into the lumped mass model here. Therefore, the shaft is separated into two different branches, an axial branch and a rotational branch, while the coupling once more is realized using constrained equations. Since all components are expressed by discrete springs and dampers, the rigidity values of shaft, coupling, and bearing are combined to an overall axial K_{ax} and rotational value K_{rot}.

In this model the inertial component parameters are defined as the following: rotary inertia of servomotor J_M, screw shaft side equivalent rotary inertia J_S, mass of base M_B, screw shaft side equivalent mass M_S, and mass of the work table M_T.

The equivalent rigidity parameters in the model are defined as the following: equivalent torsional rigidity K_{rot}, equivalent axial rigidity K_{ax}, rigidity of ball screw nut K_n, and axial rigidity of the base K_B.

The equivalent damping parameters are defined as the following: servomotor torsional damping C_M, equivalent torsional damping C_{rot}, screw shaft side damping C_S, ball screw nut damping C_n, equivalent axial damping C_{ax}, axial damping of the base C_B, and axial damping of the guide C_g.

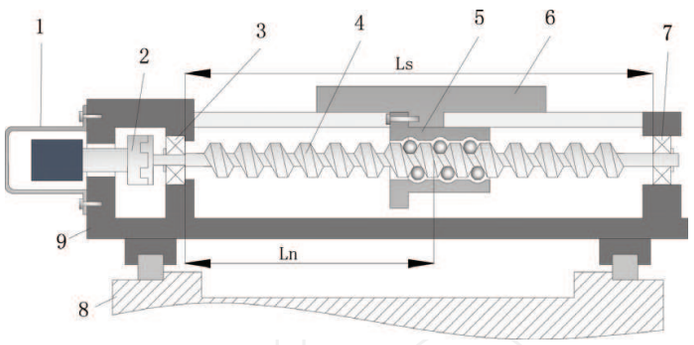

Figure 1. Typical structure of ball screw drive system. 1. Servomotor; 2. Coupling; 3. Fixed bearing; 4. Screw shaft; 5. Ball screw nut; 6. Work table; 7. Support bearing; 8. Machine bed; 9. Base.

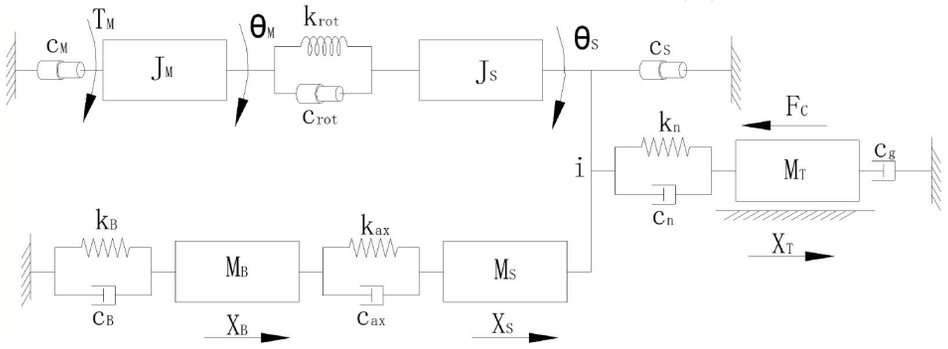

Figure 2. Lumped mass model of ball screw feed system.

The DOF parameters of the lumped mass model are defined as the following: angular rotation of the servomotor θ_M, screw shaft angular rotation at the table position θ_S, axial displacement of the base X_B, screw shaft axial displacement at the table position X_S, and work table position X_T. Therefore, the deformation of the equivalent springs is described as follows: equivalent torsional spring deformation $\theta_M - \theta_S$, equivalent axial spring deformation $X_S - X_B$, axial spring deformation of the base X_B, and screw nut contact deformation $X_T - X_S - i\theta_S$.

The speed parameters of equivalent damping are defined as the following: servomotor equivalent damping speed $\dot{\theta}_M$, equivalent torsional vibration damping speed $\dot{\theta}_M - \dot{\theta}_S$, equivalent damping speed of the screw $\dot{\theta}_S$, equivalent damping speed of the base $\dot{X}_B$, equivalent axial damping speed of screw $\dot{X}_S - \dot{X}_B$, equivalent damping speed of screw nut $\dot{X}_T - \dot{X}_S - i\dot{\theta}_S$, and speed of the work table $\dot{X}_T$.

According to the Lagrange's equations of the second kind, the dynamic model of the ball screw feed drive system is built up. The total kinetic energy T, the potential energy U, and the dissipation function of the system can be expressed using equations (2) through (4):

$$T = \frac{1}{2}J_M\dot{\theta}_M^2 + \frac{1}{2}J_S\dot{\theta}_S^2 + \frac{1}{2}M_B\dot{X}_B^2 + \frac{1}{2}M_S\dot{X}_S^2 + \frac{1}{2}M_T\dot{X}_T^2 \tag{2}$$

$$U = \frac{1}{2}k_{rot}(\theta_M - \theta_S)^2 + \frac{1}{2}k_B X_B^2 + \frac{1}{2}k_{ax}(X_S - X_B)^2 + \frac{1}{2}k_{nut}(X_T - X_S - i\theta_S)^2 \tag{3}$$

$$\begin{aligned} \mathrm{D} = {} & \frac{1}{2}C_M\dot{\theta}_M{}^2 + \frac{1}{2}C_{rot}\left(\dot{\theta}_M - \dot{\theta}_S\right)^2 + \frac{1}{2}C_S\dot{\theta}_S{}^2 + \frac{1}{2}C_B\dot{X}_B{}^2 \\ & + \frac{1}{2}C_{ax}\left(\dot{X}_S - \dot{X}_B\right)^2 + \frac{1}{2}C_n\left(\dot{X}_T - \dot{X}_S - i\dot{\theta}_S\right)^2 + \frac{1}{2}C_T\dot{X}_T{}^2 \end{aligned} \tag{4}$$

According to the definition of the system lumped mass, we have the independent coordinates system $\mathbf{q}$ as the following:

$$\mathbf{q} = (\theta_M \quad \theta_S \quad X_B \quad X_S \quad X_T)^T \tag{5}$$

The force inputs of the ball screw feed system are the servomotor torque T_M and cutting force F_C, and then the generalized forces $\mathbf{Q}$ of the system can be expressed as the following:

$$\mathbf{Q} = (T_M \quad 0 \quad 0 \quad 0 \quad -F_C)^T \tag{6}$$

With $L = T - U$, the Lagrangian function of the system about the generalized coordinate $\mathbf{q}$ and the generalized force $\mathbf{Q}$ can be calculated according to Eq. (7). Then, the matrix form of the lumped mass model of the ball screw feed system can be established as in Eq. (8):

$$\frac{d}{dt}\left(\frac{\partial L}{\partial \dot{\mathbf{q}}}\right) - \frac{\partial L}{\partial \mathbf{q}} - \frac{\partial D}{\partial \dot{\mathbf{q}}} = \mathbf{Q} \tag{7}$$

$$\mathbf{m}\ddot{\mathbf{q}} + \mathbf{c}\dot{\mathbf{q}} + \mathbf{k}\mathbf{q} = \mathbf{Q} \tag{8}$$

http://dx.doi.org/10.5772/intechopen.80716

where,

$$\mathbf{m} = \begin{bmatrix} J_M & 0 & 0 & 0 & 0 \\ 0 & J_S & 0 & 0 & 0 \\ 0 & 0 & M_B & 0 & 0 \\ 0 & 0 & 0 & M_S & 0 \\ 0 & 0 & 0 & 0 & M_T \end{bmatrix} \quad \mathrm{k} = \begin{bmatrix} k_{rot} & -k_{rot} & 0 & 0 & 0 \\ -k_{rot} & k_{rot}\text{-}i^2k_n & 0 & -ik_n & ik_n \\ 0 & 0 & k_{ax}+k_B & -k_{ax} & 0 \\ 0 & ik_n & -k_{ax} & k_{ax}+k_n & -k_n \\ 0 & -ik_n & 0 & -k_n & k_n \end{bmatrix}$$

$$\mathrm{c} = \begin{bmatrix} c_M + c_{rot} & -c_{rot} & 0 & 0 & 0 \\ -c_{rot} & c_{rot}\text{-}c_S\text{-}i^2c_n & 0 & -ic_n & ic_n \\ 0 & 0 & c_{ax}+c_B & -c_{ax} & 0 \\ 0 & ic_n & -c_{ax} & c_{ax}+c_n & -c_n \\ 0 & -ic_n & 0 & -c_n & c_n + c_g \end{bmatrix}$$

The dynamic model of the ball screw feed system shown in Eq. (8) was decomposed into three subsystems: screw shaft torsional vibration system, screw shaft axial vibration system, and the table vibration system. The simulation model of the ball screw feed system can be established as **Figure 3**. The input of the simulation model is the motor torque T_M and the cutting force F_C, and the outputs are the table acceleration a_T and displacement X_T.

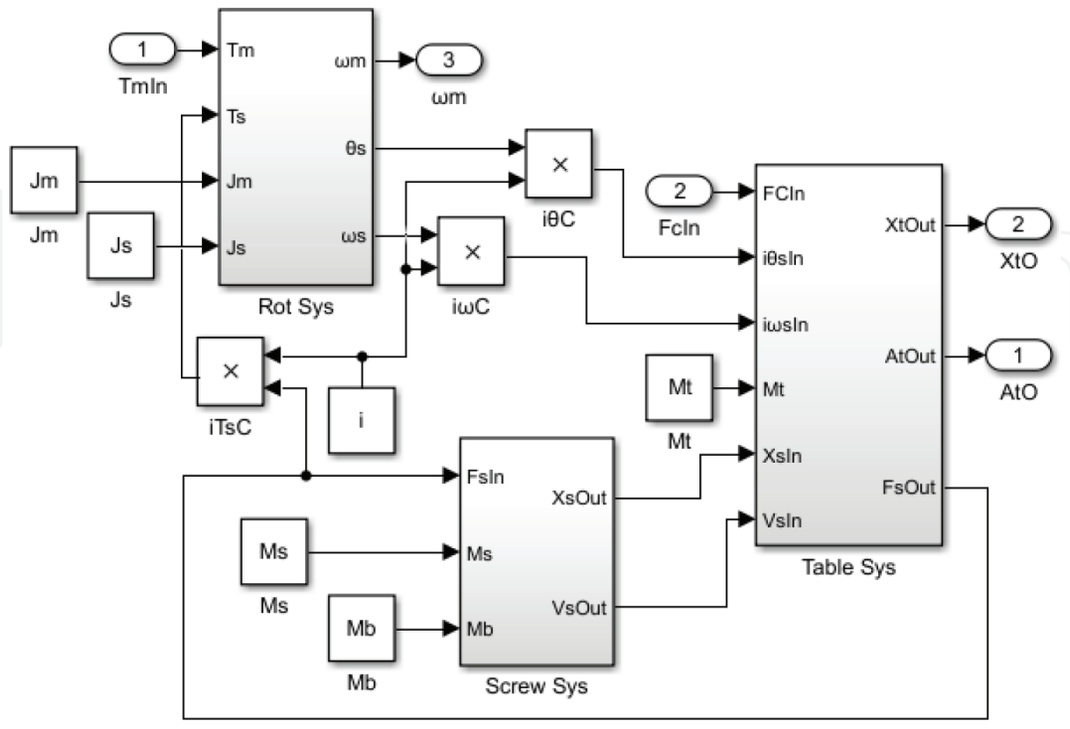

Figure 3. Simulation model of a ball screw feed drive.

2.2. Equivalent parameter calculation method of ball screw feed system lumped mass model

Accurate ball screw feed system dynamic model requires a reasonable equivalent parameter calculation method of the lumped mass model. As mentioned the shaft has influence on the rotational mode and the axial mode of the drive system; the shaft is separated into two different branches, an axial branch and a rotational branch, while the coupling is realized using constrained equations. The dynamic characteristics of the feed system should be analyzed to select the appropriate equivalent parameter calculation method. The inertia of the axial system and the inertia of rotational system are not only the mass or inertia of the component itself but also the mass or inertia converted to the independent coordinate system component of the dynamic system.

The equivalent rotary inertia of the screw J_S is composed of the rotary inertia of the screw J_{sc}, the rotary inertia of the coupling J_c, and the mass of the table M_T converted to the rotary inertia of the screw:

$$J_S = J_{sc} + J_c + M_T i^2 \tag{9}$$

With the material density ρ, namely, equivalent diameter d_s and length l_s of the screw shaft, the rotary inertia of the screw J_{sc} can be approximated using the following equation:

$$J_{sc} = \frac{\rho \cdot \pi}{32} d_s^4 l_s \tag{10}$$

The screw equivalent mass M_S is composed of screw mass M_{sc}, servomotor rotor mass M_m, and coupling mass M_c; with the material density ρ, namely, equivalent diameter d_s and length l_s of the screw shaft, the rotary inertia of the screw values J_{sc} can be approximated using the following equations:

$$M_S = M_{sc} + M_m + M_c \tag{11}$$

$$M_{sc} = \frac{\rho\pi}{4} d_s^2 l_s \tag{12}$$

The axial rigidity of the ball screw feed system is related to the installation method of the screw. Here is an example of the screw-fixed-support method used on most machine tools (**Figure 4**). Servomotor side of the screw shaft uses fixed support to provide screw axial support, and the end of the shaft is free support. Therefore, the axial rigidity k_{ax} of the ball

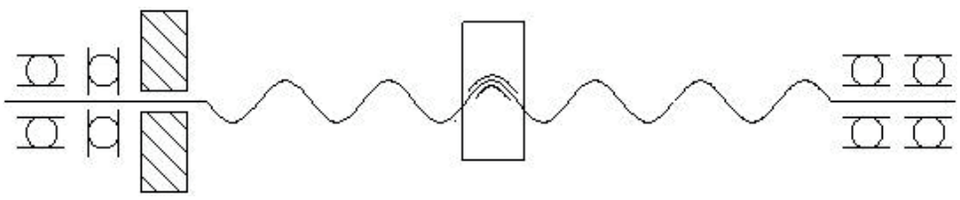

Figure 4. Screw fixation-support installation diagram.

screw feed system consists of screw bearing rigidity k_b, and the axial rigidity of the screw shaft $k_{s_{ax}}$ is as follows:

$$k_{ax} = \left(\frac{1}{k_b} + \frac{1}{k_{s_{ax}}}\right)^{-1} \tag{13}$$

With the material elastic modulus E, screw cross-sectional area A, and ball screw length at table position l_n, the axial rigidity of the screw according to the position of the table $k_{s_{ax}}$ can be established as shown in Eq. (14):

$$k_{s_{ax}} = \frac{EA}{l_n} = \frac{\pi d_s^2 E}{4 l_n} \tag{14}$$

The torsional rigidity of the ball screw feed system k_{rot} consists of the torsional rigidity of the screw $k_{s_{rot}}$ and the torsional rigidity of the coupling k_c. According to the position of the table, the torsional rigidity of the screw $k_{s_{rot}}$ can be approximated with the shear modulus G and polar rotary inertia of the screw section I_P as shown in Eq. (16):

$$k_{rot} = \left(\frac{1}{k_c} + \frac{1}{k_{s_{rot}}}\right)^{-1} \tag{15}$$

$$k_{s_{rot}} = \frac{T}{\Delta\theta} = \frac{G \cdot I_P}{l_n} = \frac{G \cdot \pi \cdot d_s^4}{32 \cdot l_n} \tag{16}$$

With the nut reference rigidity K, nut axial load F_a, and basic dynamic load C_a, the contact rigidity of the screw nut k_n can be expressed as follows:

$$k_n = 0.8K\left(\frac{F_a}{0.1C_a}\right)^{\frac{1}{3}} \tag{17}$$

3. Servo control system modeling and simulation

3.1. Modeling of permanent magnet synchronous motor

Permanent magnet synchronous motors can be divided into two types according to the rotor type, salient pole rotor and non-salient pole rotor. The structure is shown in **Figure 5**; in the surface-mounted permanent magnet synchronous motor (**Figure 5(a)**), the magnetic circuit of the rotor is symmetrical, and the magnetic permeability and air gap permeability of the permanent magnet material are approximately the same. In the rotor two-phase coordinate system, the direct-axis inductance and the quadrature-axis inductance are equal, that is $L_d = L_q$. It is named non-salient pole rotor permanent magnet synchronous motor.

The rotor magnetic paths of plug-in-type (**Figure 5(b)**) and built-in-type (**Figure 5(c)**) permanent magnet synchronous motors are asymmetrical, and the quadrature-axis inductance is

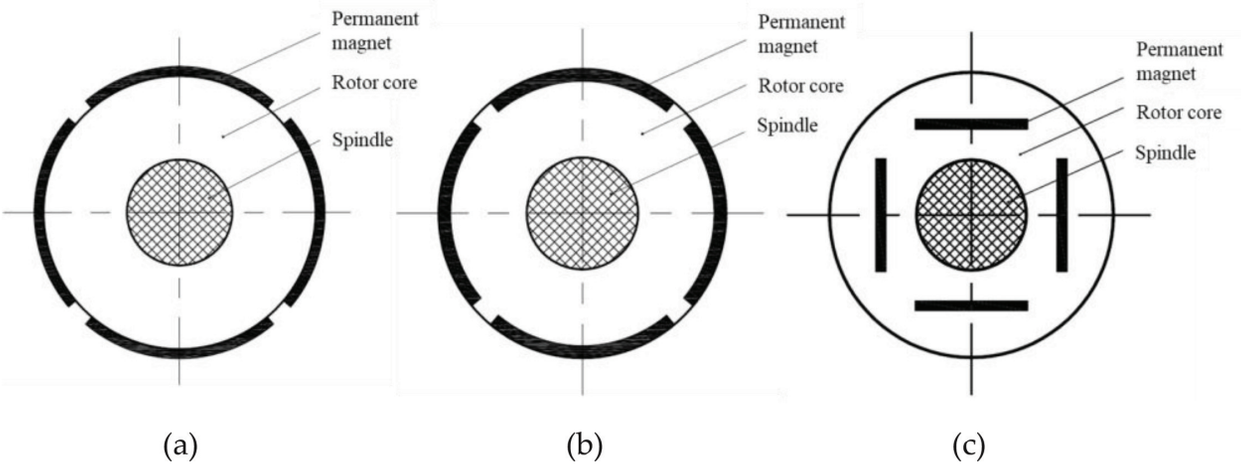

Figure 5. PMSM motor rotor structure. (a) Surface-mounted; (b) Plug-in; and (c) Interior-mounted.

greater than the direct-axis inductance, that is $L_q > L_d$. The rotor shows salient pole effect, which is called salient pole-type permanent magnet synchronous motor.

Taking non-salient pole rotor permanent magnet synchronous motor as an example, we simplify the motor model with the following conditions: neglecting the saturation of the motor core; no eddy current and hysteresis loss; permanent magnet material has zero conductivity; three-phase windings are symmetrical; and induced potential in the winding is sinusoidal. Then, a schematic diagram of the physical model of the motor shown in **Figure 6** can be obtained.

The axis of the sinusoidal magnetomotive wave generated by a flowing forward current through the phase winding is defined as the axis of the phase winding. Take axis A as the spatial reference coordinate of the ABC coordinate system. It is assumed that the positive direction of the induced electromotive force is opposite to the positive direction of the current (motor principle); take the counterclockwise direction as the positive direction of the speed and

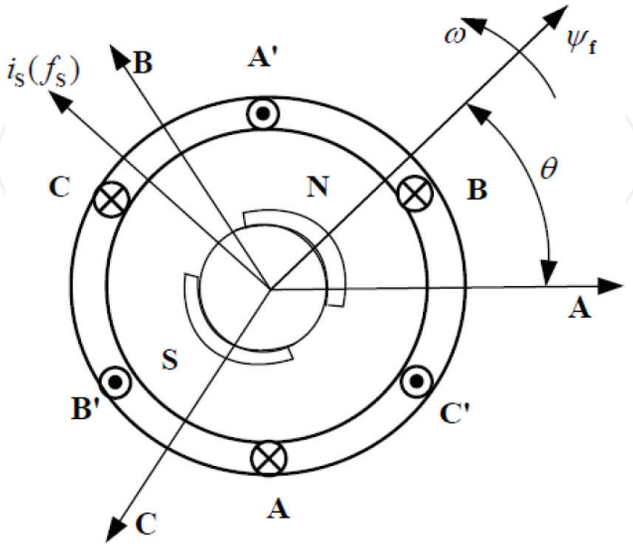

Figure 6. PMSM physical model.

electromagnetic torque, and the positive direction of the load torque is the opposite. The physical model equation of permanent magnet synchronous motor is as follows:

$$\begin{cases} U_S = Ri_s + \dfrac{d\Psi_s}{dt} \\ \Psi_s = Li_s + \Psi_f \begin{bmatrix} \cos(\theta + \omega t) \\ \cos(\theta + \omega t + 2\pi/3) \\ \cos(\theta + \omega t - 2\pi/3) \end{bmatrix} \end{cases} \tag{18}$$

$$\begin{bmatrix} u_A \\ u_B \\ u_C \end{bmatrix} = \begin{bmatrix} R & 0 & 0 \\ 0 & R & 0 \\ 0 & 0 & R \end{bmatrix} . \begin{bmatrix} i_A \\ i_B \\ i_C \end{bmatrix} + \begin{bmatrix} \dfrac{d\varphi_A(\theta, i)}{dt} \\ \dfrac{d\varphi_A(\theta, i)}{dt} \\ \dfrac{d\varphi_A(\theta, i)}{dt} \end{bmatrix} \tag{19}$$

In Formula (18), R and L are matrices and their expressions are shown in Formula (20):

$$\begin{cases} U_s = [\, U_A \quad U_B \quad U_C \,]^T \\ i_s = [\, i_A \quad i_B \quad i_C \,]^T \\ R = \begin{bmatrix} R_S & 0 & 0 \\ 0 & R_S & 0 \\ 0 & 0 & R_S \end{bmatrix} \\ L = \begin{bmatrix} L_A & M_{AB} & M_{AC} \\ M_{BA} & L_B & M_{BC} \\ M_{CA} & M_{CB} & L_C \end{bmatrix} \end{cases} \tag{20}$$

U_A, U_B, and U_C are phase voltages of PMSM stator three-phase windings. I_A, I_B, and I_C are the phase currents of stator three-phase windings. R_S is the stator winding value. L_A, L_B, and L_C are stator winding self-inductances. $M_{AB} = M_{BA}$, $M_{AC} = M_{CA}$, and $M_{BC} = M_{CB}$ are the stator winding mutual inductances.

3.2. Coordinate transformation

From the above physical model, we can see that in the ABC coordinate system, the PMSM rotor is asymmetric in the magnetic and electrical structures. The motor equation is a set of nonlinear time-varying equations related to the instantaneous position of the rotor, which makes the analysis of the dynamic characteristics of the PMSM very difficult. It is usually necessary to convert the motor equations by coordinate transformation to facilitate analysis and calculation. The coordinate system used in the vector control of the permanent magnet synchronous motor and their relationship is shown in **Figure 7**. In the figure, the $\alpha - \beta$

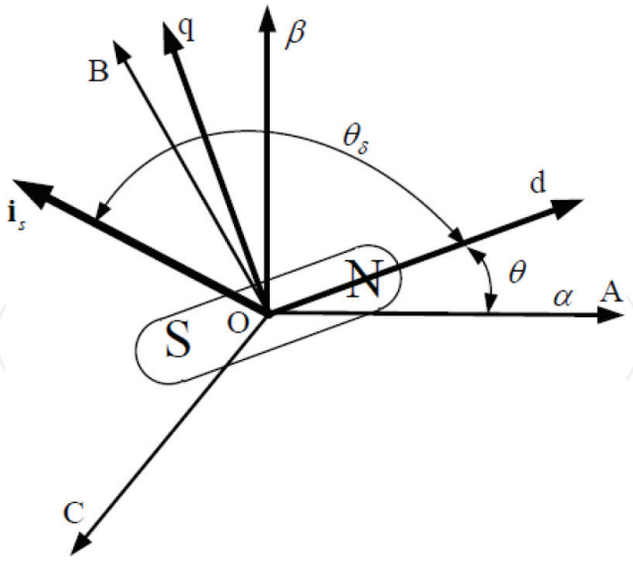

Figure 7. The coordinate system used in the vector control and their relationship.

coordinate system is a two-phase stationary coordinate system, and the $d-q$ coordinate system is a two-phase rotating coordinate system that is fixed to the rotor.

3.2.1. Clarke transformation

Clarke transformation simplifies the voltage loop equations on the original three-phase windings into the voltage loop equations on the two-phase windings, from the three-phase stator ABC coordinate system to the two-phase stator $\alpha-\beta$ coordinate system, as shown in Eq. (21); its inverse transform is shown in Eq. (22). However, after the Clarke transformation, the torque still depends on the rotor flux. In order to facilitate control and calculation, Park transformation is also required:

$$\begin{bmatrix} i_\alpha \\ i_\beta \end{bmatrix} = \sqrt{\frac{2}{3}} \begin{bmatrix} 1 & -1/2 & -1/2 \\ 0 & \sqrt{3}/2 & -\sqrt{3}/2 \end{bmatrix} \begin{bmatrix} i_A \\ i_B \\ i_C \end{bmatrix} \tag{21}$$

$$\begin{bmatrix} i_A \\ i_B \\ i_C \end{bmatrix} = \sqrt{\frac{3}{2}} \begin{bmatrix} 1 & 0 \\ -1/2 & \sqrt{3}/2 \\ -1/2 & -\sqrt{3}/2 \end{bmatrix} \begin{bmatrix} i_\alpha \\ i_\beta \end{bmatrix} \tag{22}$$

3.2.2. Park transformation

In the physical sense, the Park transformation is equivalent to projecting the currents i_a, i_b, i_c onto the $d-q$ axis. The transformed coordinate system rotates at the same speed as the rotor, and the d-axis and the rotor flux have the same position. The Park transformation is shown in Eq. (23), and the inverse transformation is shown in Eq. (24). This transformation also holds for the three-phase voltage and flux linkage:

$$\begin{bmatrix} i_d \\ i_q \end{bmatrix} = \begin{bmatrix} \cos\theta & \sin\theta \\ -\sin\theta & \cos\theta \end{bmatrix} \begin{bmatrix} i_\alpha \\ i_\beta \end{bmatrix} \tag{23}$$

$$\begin{bmatrix} i_\alpha \\ i_\beta \end{bmatrix} = \begin{bmatrix} \cos\theta & -\sin\theta \\ \sin\theta & \cos\theta \end{bmatrix} \begin{bmatrix} i_d \\ i_q \end{bmatrix} \tag{24}$$

3.2.3. Mathematical model of permanent magnet synchronous motor in coordinate system

The mathematical model of the permanent magnet synchronous motor in the ABC coordinate system can be transformed into any two-phase coordinate system through coordinate transformation, so that it is possible to simplify the decoupling of the motor flux linkage equation and the electromagnetic torque equation. If the mathematical model of the motor is transformed into a $d-q$ coordinate system fixed on a permanent magnet rotor, the motor flux equation and the electromagnetic torque equation will be greatly simplified.

With the equivalent flux ψ_d and ψ_q, the equivalent inductance L_d, L_q of the motor in the $d-q$ coordinate system, and the rotor permanent magnet flux linkage ψ_f, the stator flux equation can be obtained in Eq. (25):

$$\begin{cases} \psi_d = L_d i_d + \psi_f \\ \psi_q = L_q i_q \end{cases} \tag{25}$$

Take the rotor permanent magnet flux linkage ψ_f as constant; the voltage of stator in the $d-q$ coordinate system is as follows:

$$\begin{cases} u_d = R i_d + L_d \dfrac{di_d}{dt} - \omega_r L_q i_q \\ u_q = R i_q + L_q \dfrac{di_q}{dt} + \omega_r L_d i_d + \omega_r \psi_f \end{cases} \tag{26}$$

where u_d and u_q are the stator-side equivalent voltages of the motor in the $d-q$ coordinate system, R is the stator winding resistance per phase, and ω_r is the electrical angular velocity of the rotor rotation.

The electromagnetic torque equation in the $d-q$ coordinate system can be expressed as follows, where p is the number of pole pairs, $\boldsymbol{\psi}$ is the flux synthesis vector, and $\mathbf{i}$ is the current composition vector:

$$T_e = 1.5p\boldsymbol{\psi} \times \mathbf{i} \tag{27}$$

Using the components of the $d-q$ coordinate system to represent the flux linkage and current vector shown in Eq. (28), the electromagnetic torque can be expressed as shown in Eq. (29):

$$\begin{cases} \mathbf{i} = i_d + j i_q \\ \boldsymbol{\psi} = \psi_d + j\psi_q \end{cases} \tag{28}$$

$$T_e = 1.5p\left[\psi_f i_q + \left(L_d - L_q\right) i_d i_q\right] \tag{29}$$

3.3. Servo control modeling of ball screw feed system

In order to model the servo control of the ball screw feed system, the modeling of the three-loop cascade control architecture of the vector control and servo control system of the permanent magnet synchronous servomotor is studied, which is commonly used in the ball screw feed system.

3.3.1. Modeling of permanent magnet synchronous motor vector control.

The principle of space vector pulse width modulation (SVPWM) is based on vector equivalents. The magnitude and direction of the current vector can be indirectly controlled by the timing of the six switching elements of the inverter through the three-phase winding of the permanent magnet synchronous motor, so that the winding produces a constant amplitude circular magnetic field that rotates according to a given demand, thus dragging the permanent magnet to rotate. The voltage inverter circuit is shown in **Figure 8**. The simulation model of SVPWM control system for permanent magnet synchronous motor is shown in **Figure 9**.

3.3.2. Modeling of cascade control system

The SVPWM control system for permanent magnet synchronous motor is based on the three-phase current information and rotor position information fed back by the motor. AC motor is equivalent to a direct current motor by formula transformation to control the position and amplitude of the stator current.

The control system schematic is shown in **Figure 10(a)**. The system includes a cascaded control structure with a P-position controller, a PI-velocity controller, and a PI-current controller. In the cascade control system, the servomotor feedback speed ω_M and the work table feedback

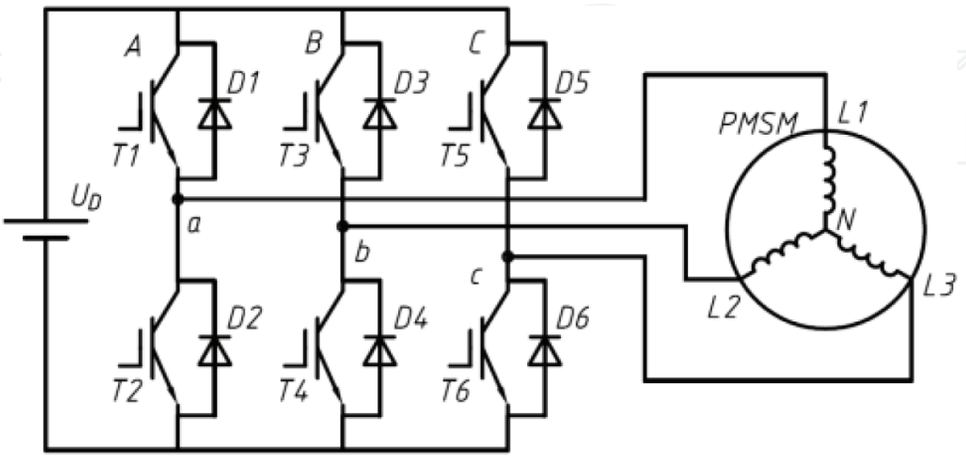

Figure 8. Circuit of voltage bridge inverter.

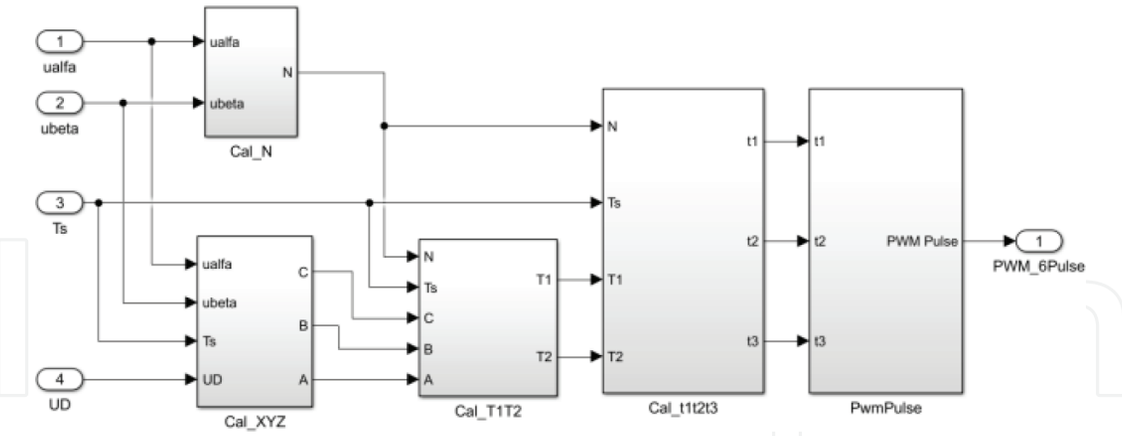

Figure 9. Simulation model of SVPWM control system.

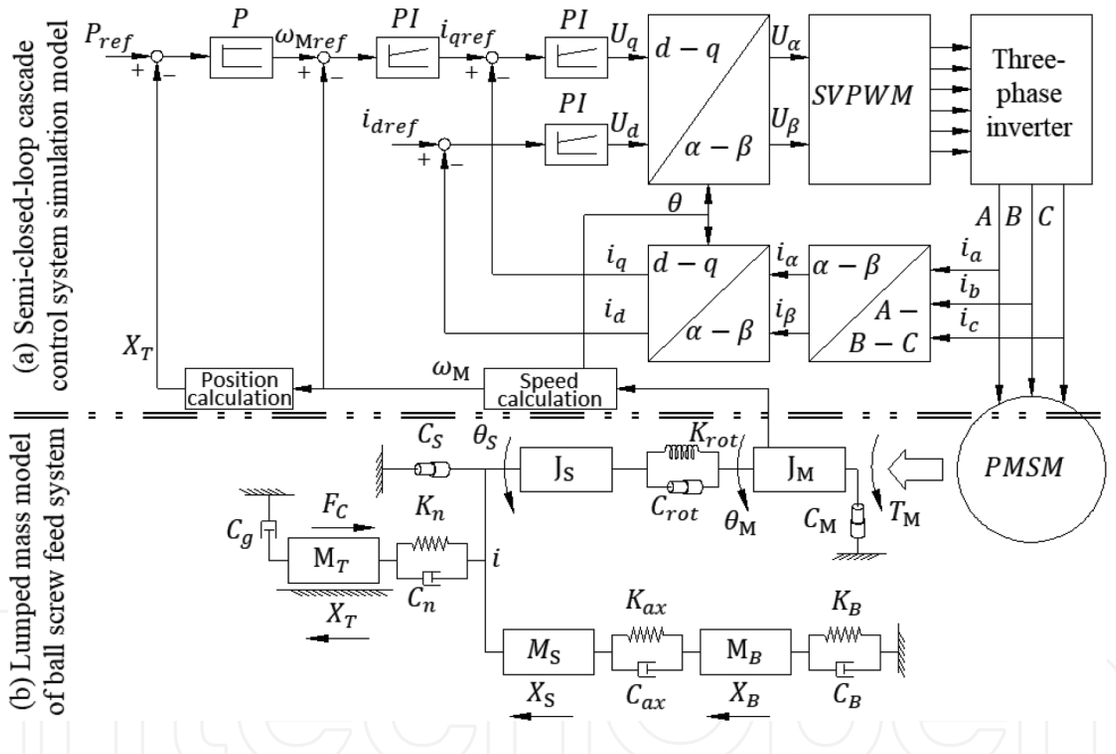

Figure 10. Schematic of ball screw feed drive system electromechanical co-simulation.

position X_T are calculated by the rotor position detected by the encoder on the servomotor. The input P_{ref} is given by the CNC system according to the feed motion command, the input P_{ref} and work table feedback position X_T are compared, and the reference speed ω_{Mref} is given by the position controller. Then, the reference speed ω_{Mref} is compared with the feedback speed ω_M, and the velocity controller gives the reference current i_{qref} for the q-axis and the reference current $i_{dref} = 0$ for the d-axis of the stator. The three-phase current of the servomotor is detected and converted into i_d and i_q in $d - q$ coordinate system through the Clark and Park

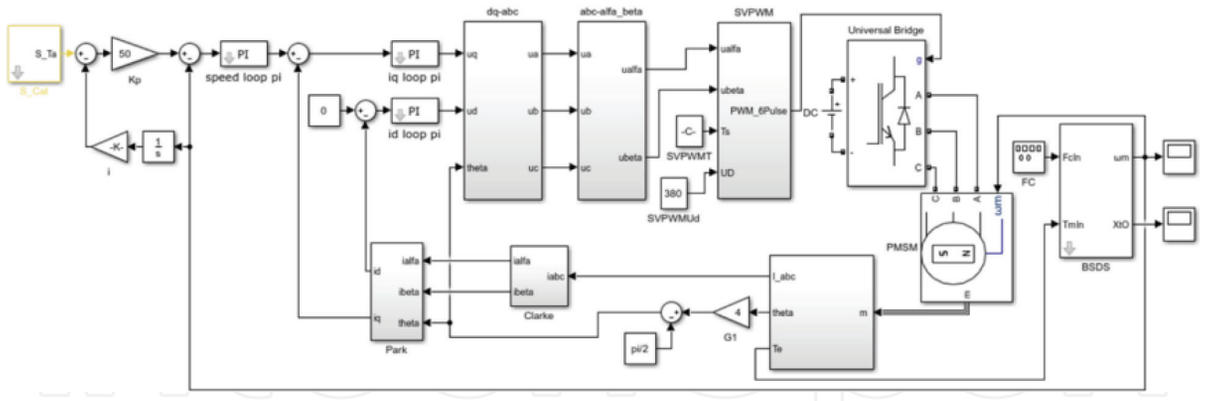

Figure 11. Electromechanical co-simulation model of half-closed ball screw feed system.

transformation. i_{dref} and i_{qref} are compared with the feedback i_d and i_q, respectively, and the current controller calculates the given voltages U_d and U_q of the d and q axes; then, they are converted into U_α and U_β in the $\alpha - \beta$ coordinate system by Park inverse transformation. Finally, the SVPWM module generates six-phase PWM to drive the three-phase inverter. The inverter outputs ABC three-phase voltage to servomotor stator, which generates rotating magnetic field and produces magnetic torque on the servomotor rotor. This magnetic torque is the output torque T_M of the servomotor and drives the rotor to rotate under the dynamic relations of ball screw feed system.

3.4. Electromechanical co-simulation modeling of ball screw feed drive system

Based on the lumped mass model of ball screw feed system and the servo control system simulation model, an electromechanical co-simulation model of the ball screw feed drive system was constructed. The co-simulation schematic is shown in **Figure 10**; as described above (a) is the semi-closed-loop cascade control system simulation model, while (b) is the lumped mass model of ball screw feed system. The inverter outputs ABC three-phase voltage to servomotor stator, which generates rotating magnetic field and produces magnetic torque on the servomotor rotor. This magnetic torque is the output torque T_M of the servomotor and drives the rotor to rotate under the dynamic relations as shown in Eq. (8).

The electromechanical co-simulation model of the ball screw feed drive system is shown in **Figure 11**. The S_Cal module on the left side generates the trajectory command for the feed drive system according to the acceleration/deceleration strategy. Under the cascade control system, which consists of position controller, velocity controller, and current controller, the servomotor drive and the ball screw accomplish the motion command accordingly.

4. Experimental verification of the electromechanical co-simulation model of ball screw feed drive system

The electromechanical co-simulation model in this chapter has been tested on a single-axis ball screw drive system test bench shown in **Figure 12**. The test bench uses an i5 CNC system and

http://dx.doi.org/10.5772/intechopen.80716

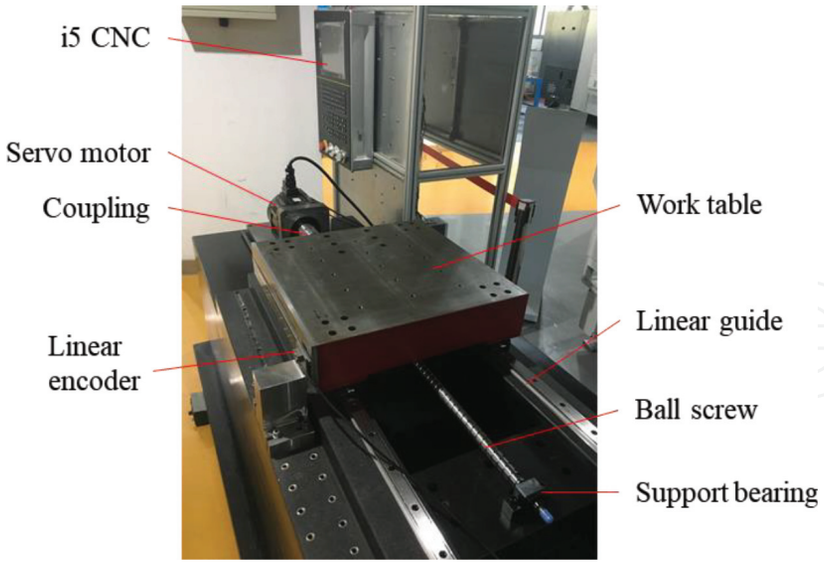

Figure 12. Single-axis ball screw feed drive test bench.

servo system of Shenyang Machine Group, which use a semi-closed-loop cascade control structure. The specifications of the test bench are listed in **Table 1**, which are either obtained from the manufacturers' catalogs, approximated from prior knowledge, or calculated from computer-aided design (CAD). According to the modeling method described in Chapter 2, the lumped mass model of this ball screw feed system test bench was built up. The equivalent parameters of the lumped mass model were calculated by using the specifications in **Table 1**, and the other calculated lumped parameters are listed in **Table 2**.

Taking the servomotor torque as input and the axial acceleration of work table as output, the frequency response characteristics of the lumped parameter model of the test bench are analyzed. The bode diagram is shown in **Figure 13**, and simulation result shows that the work table has four-order natural frequencies, which are 26.2, 76.7, 247, and 633 Hz. Further study shows that 76.7 Hz is the main axial vibration frequency of the work table, 26.2 Hz is the main axial vibration frequency of the base, and 247 and 633 Hz are the rotational vibration frequencies.

Parameter of the component	Value	Parameter of the component	Value
Work table mass M_T (kg)	206	Rotary inertia of coupling J_C $(kg \cdot m^2)$	1.09×10^{-4}
Base mass M_B (kg)	3820	Rotary inertia of motor J_M $(kg \cdot m^2)$	6.75×10^{-3}
Coupling mass M_c (kg)	1.18	Torsional rigidity of coupling k_c (N/m)	1.4×10^3
Motor rotor mass M_m (kg)	10.9	Screw bearing rigidity k_b (N/m)	1×10^8
Screw pitch length h (m)	1.6×10^{-2}	Nut reference rigidity K (N/m)	6.12×10^8
Screw diameter d_s (m)	2.5×10^{-2}	Nut basic dynamic load C_a (N)	37.4
Screw length l_s (m)	1	Ball screw length at table position l_n (m)	0.35

Table 1. Specifications of the test bench.

Parameter of the component	Value	Parameter of the component	Value
Screw equivalent mass M_S (kg)	11.28	Equivalent rotary inertia of screw J_S $(kg \cdot m^2)$	1.7×10^{-3}
Axial rigidity of screw K_{ax} (N/m)	0.743×10^8	Rotary rigidity of screw K_{rot} $(N \cdot m \cdot rad^{-1})$	3.14×10^3
Axial rigidity of base K_B (N/m)	1×10^8	Contact rigidity of the screw nut K_n (N/m)	9.8×10^7

Table 2. Calculated parameters used in the lumped mass model of test bench.

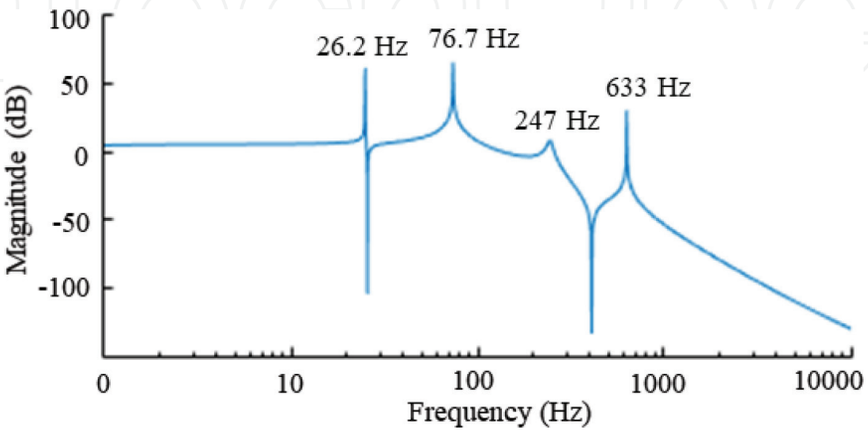

Figure 13. Bode diagram of the lumped parameter model of ball screw feed system.

To establish the simulation model of servo control system, the servomotor parameters are needed as shown in **Table 3**.

In order to compare and verify the simulation results with the experimental results, the motion command parameters and the control parameters of the experimental test and simulation are set in **Table 4**.

Parameter name	Value	Parameter name	Value
Rated power (kW)	4.4	Number of pole pairs	4
Rated torque $(N \cdot m)$	18.6	Stator resistance per phase (Ω)	1.44
Rotor inertia $(kg \cdot m^2)$	6.75×10^{-3}	Inductance L_d, L_q (H)	8.15×10^{-3}
Rated speed (r/min)	1500	Permanent magnetic flux $\psi_f(wb)$	0.21

Table 3. Parameters of the servomotor.

Parameter name	Value	Parameter name	Value
Position instruction (mm)	400	Position loop gain k_p	50
Maximum velocity (mm/s)	400	Velocity loop gain k_v	10
Maximum acceleration (mm/s^2)	2000	Current loop gain k_i	30
Maximum jerk (mm/s^3)	20,000		

Table 4. Motion command parameters and the control parameters settings.

http://dx.doi.org/10.5772/intechopen.80716

Using the same operation parameters as set in the simulation model, a feed motion experiment was conducted and the work table position was measured. The simulation results are compared to the experimental results. **Figures 14** and **15** exemplarily show simulated and measured

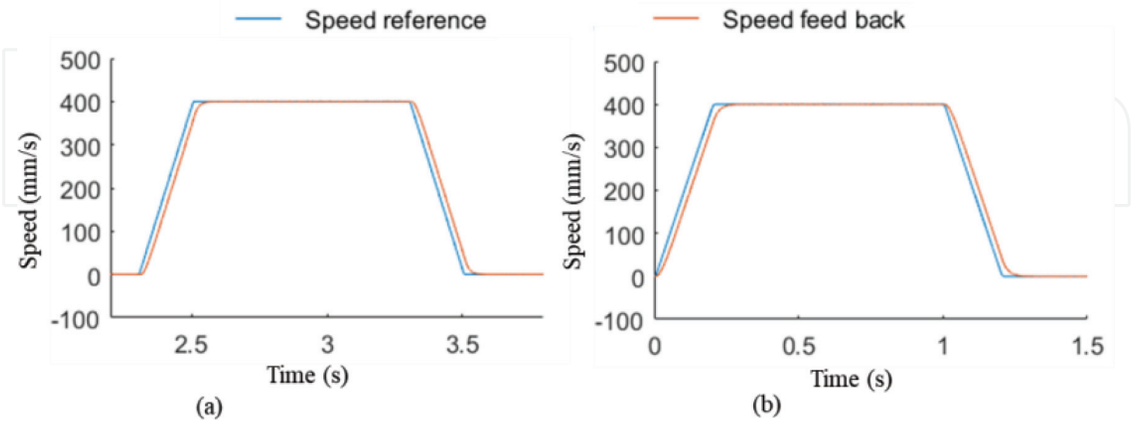

Figure 14. Reference velocity and feedback velocity.

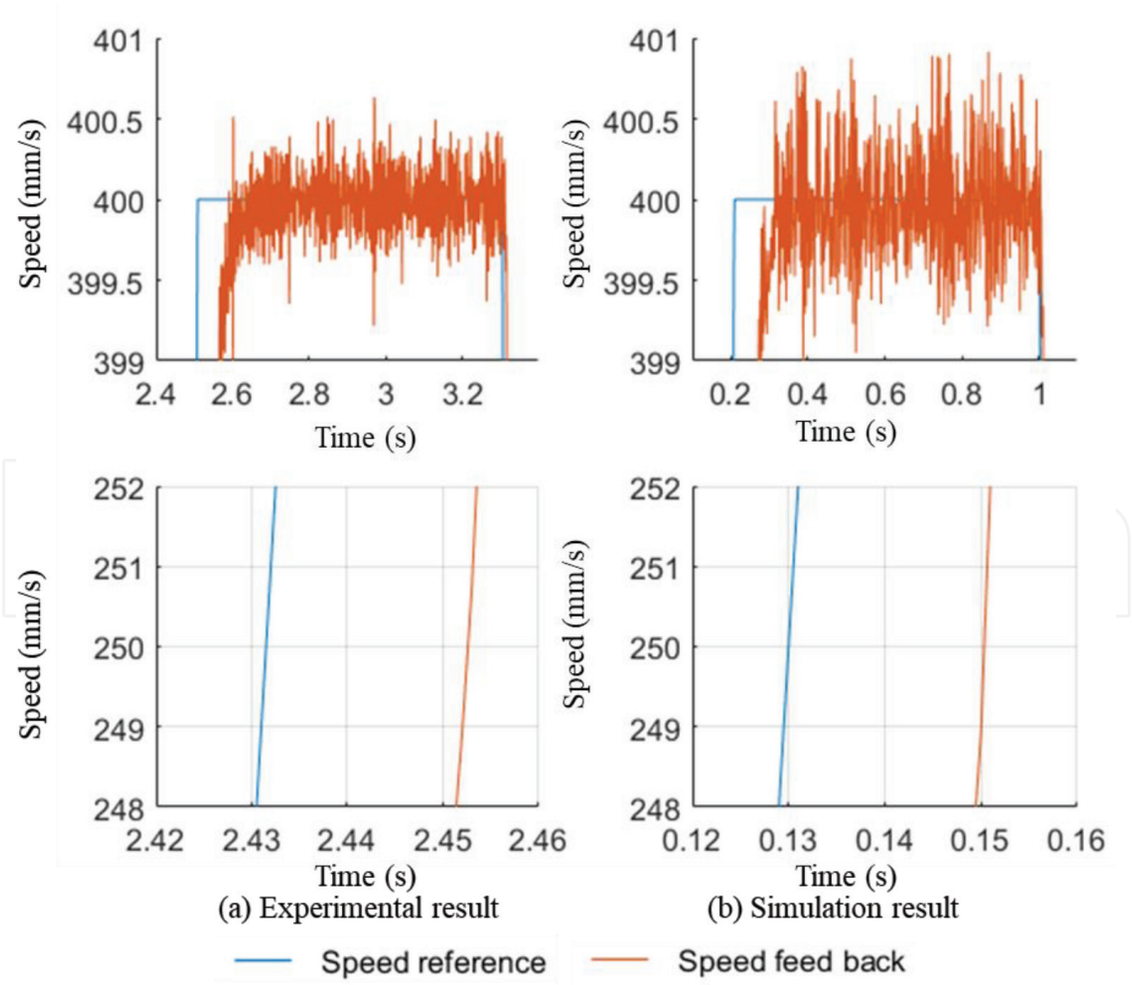

Figure 15. Detailed reference velocity and feedback velocity.

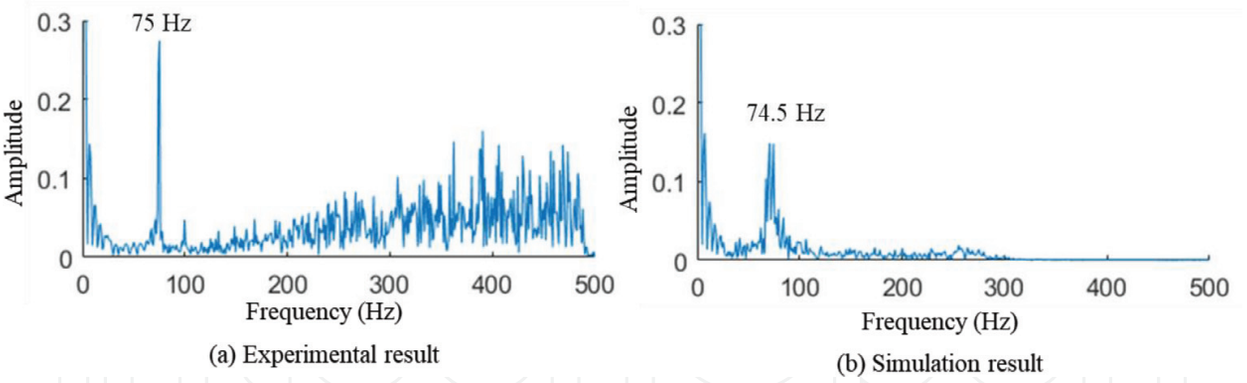

Figure 16. Frequency contents of work table acceleration.

reference velocity and feedback velocity of the servomotor at the given operating conditions. The simulation result has a similar curve to the experimental result.

Figure 16 shows frequency contents of the work table acceleration signals from simulation result and the experimental result. Comparing the simulation result with the experimental result, the co-simulation model of ball screw feed drive system can predict the vibration that occurs in the feed operation. Both results show that in this case the second-order natural frequency (about 75 Hz) but not the first-order natural frequency is the main factor influencing the performance of feed drive system.

5. Conclusions

In this chapter an electromechanical co-simulation model of the ball screw feed drive system was constructed based on lumped mass model of ball screw feed system and the servo control system simulation model, which can be used to study the dynamic characteristics and vibration behavior of the feed drive system. Simulative and experimental tests were conducted based on a ball screw feed drive system test bench. The result shows that the co-simulation model of ball screw feed drive system can predict the vibration that occurs in the feed operation. Because of the integration of lumped parameter model into the detailed modeled cascade control simulation model, the electromechanical co-simulation of ball screw feed drive system could achieve a very good predictability for control performance and vibration behavior study of ball screw feed drive system, which may be affected by the servo controller, ball screw feed system, or the coupling between them.

Acknowledgements

This work is supported by the major national science and technology projects “high-end CNC machine tools and basic manufacturing equipment” (2012ZX04005031).

Author details

Liang Luo and Weimin Zhang*

*Address all correspondence to: iamt.tongji.edu.cn

School of Mechanical Engineering, Tongji University, Shanghai, China

References

[1] Altintas Y, Verl A, et al. Machine tool feed drives. CIRP Annals–Manufacturing Technology. 2011;**60**:779-796

[2] Verl A, Frey S. Improvement of feed drive dynamics by means of semi-active damping. CIRP Annals–Manufacturing Technology. 2012;**61**:351-354

[3] Dietmair A, Verl A. Drive based vibration reduction for production machines. Science Journal. 2009, Oct:130-134

[4] Ming Y, Hao H, Dianguo X. Cause and suppression of mechanical resonance in PMSM servo system. Electric Machines and Control. 2012, Jan;**16**(1):79-84

[5] Jian-Ren S. Research on ACC/DEC Control and Contour Error of CNC System. Lan Zhou: Lanzhou University of Technology; 2012

[6] Erkorkmaz K, Altintas Y. High speed CNC system design. Part I: Jerk limited trajectory generation and quintic spline interpolation. International Journal of Machine Tools and Manufacture. 2001;**41**(9):1323-1345

[7] Sato R. Development of a feed drive simulator. Key Engineering Materials. 2012;**516**: 154-159

[8] Frey S, Dadalau A, Verl A. Expedient modeling of ball screw feed drives. Production Engineering. 2012;**6**(2):205-211

[9] Okwudire EC, Altintas Y. Hybrid modeling of ball screw drives with coupled axial, torsional and lateral dynamics. Journal of Mechanical Design. 2009;**131**:071002-1-071002-9

[10] Liang L, Weimin Z, Mingjian Z, et al. Dynamics modeling and simulation of ball screw feed drive based on lumped mass model. Transactions of the Chinese Society for Agricultural Machinery. 2015;**46**(12):370-377

IntechOpen